Analysis of frequency selective surface absorbers via a novel equivalent circuit method*

Liu Li-Guo(刘立国)†, Wu Wei-Wei(吴微微), Mo Jin-Jun(莫锦军),
Fu Yun-Qi(付云起), and Yuan Nai-Chang(袁乃昌)

College of Electronic Science and Engineering, National University of Defense Technology, Changsha 410073, *China*

(Received 7 October 2012; revised manuscript received 2 December 2012)

An equivalent circuit (EC) method for absorbers design is proposed in this paper. Without using full-wave analysis, the EC method can predict the performance of the absorbers. This method is employed to synthesize broadband absorbers by inserting the resistors respectively into the single- and double-square loops structures, then two different prototypes with broadband absorbing frequency bands are manufactured and measured. By comparisons with the results both by using the full-wave analysis and by the measurements, the correctness of the new EC method is verified. Some factors which affect the absorbing bandwidth are also investigated. Due to its fast and accurate characteristics, the EC method which can be theoretically applied to arbitrary FSS is a good candidate for broadband design of the absorbers.

Keywords: frequency selective surfaces, equivalent circuit, absorber

PACS: 78.20.Ci, 41.20.Jb **DOI:** 10.1088/1674-1056/22/4/047802

1. Introduction

During the last decades, intensive attention[1–4] was turned to the research on the frequency selective surfaces (FSS) which serve as a filter for the plane wave. Its applications include frequency separation[5] in quasi-optical beam splitters, the provision of windows in metallic radomes,[6] and so on. In recent years, electromagnetic band gap materials[7,8] and metamaterial absorbers[9–12] have been suggested to construct an ultra-thin absorber. The researchers employed them to improve the performance of classic electromagnetic absorbers. By inserting chip resistors into the structures of single- and double-square loops,[13] this kind of structure can perform great wideband absorption due to Ohmic loss introduced by lumped resistors. They can be used as radar absorbers for their thin and low-cost characteristics.

The design of these structures is usually achieved by full-wave analysis such as MoM and FDTD codes. The advantage of this method is its universality and accurateness for arbitrary FSS configuration. However, this method is time-consuming. A quasi-equivalent circuit approach[14] was proposed in which the full-wave analysis was applied to compute the impedance of the FSS. Furthermore, an analysis of absorbers comprising resistively loaded high impedance surfaces was executed.[15] In order to get the characteristics of the configurations more quickly, a thorough equivalent circuit (EC) method without using full-wave analysis is presented. In theory, our method can be expanded for arbitrary FSS absorbers.[16] In this paper, absorbers of single- and double-square loops are analyzed via this method. By comparisons with the results obtained both by full-wave analysis and by the measurements, the correctness of our method is validated. Due to its fast and accurate characteristics, the EC method can be a good candidate for designing the absorbers.

2. Equivalent circuit model

2.1. Impedance calculation of metallic FSS

Marcuvitz[17] first developed the analytic expressions for periodic grating. Anderson[18] was the first man to apply this technology to FSS. Langley *et al.*[19–21] applied it to the Jerusalem cross FSS as well as both single- and double-square loops FSS. An improved model[22] was developed at oblique angles for both TE- and TM-incidences. These efforts are devoted to designing the FSS. However, by inserting the lumped resistors, the periodic structure shown in Fig. 1(a) and Fig. 1(b) can be used not only as a filter but also as the absorbers. The equivalent circuit models of the single- and double-square loops are proposed, shown in Fig. 2(a) and Fig. 2(b) respectively.

The absorbers consist of metallic FSS loaded with lumped resistors over the grounded dielectric slab, shown in Fig. 3(a). The parallel circuit is applied to extract the characteristics of each unit of the absorbers. The metallic FSS loaded with lumped resistors can be approximated by a series RLC circuit with the total impedance $Z_{\rm FSS}$. The transmission line's impedance can be expressed by Z_m. The equivalent circuit of the absorbers is given in Fig. 3(b).

*Project supported by the Science Foundation for New Century Excellent Talents in University of China (Grant No. NCET-10-0894).
†Corresponding author. E-mail: liguoliu99@gmail.com
© 2013 Chinese Physical Society and IOP Publishing Ltd

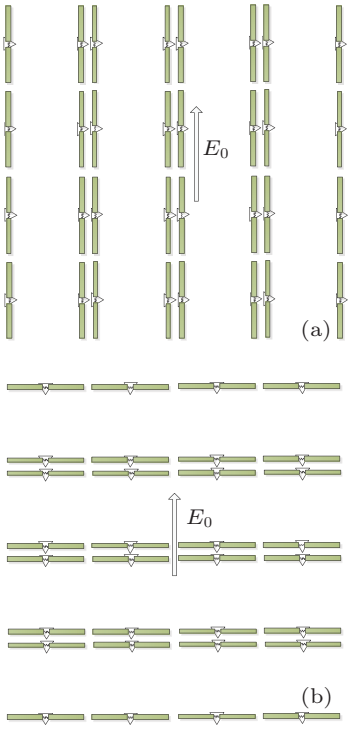


Fig. 1. (color online) The sketch of the absorbers. (a) Arms parallel to the electric field, and (b) arms perpendicular to the electric field.

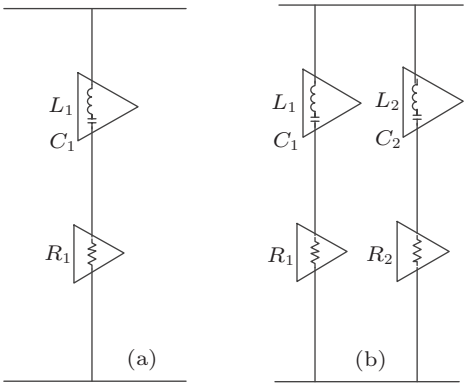


Fig. 2. (a) Equivalent circuit of the single-loop, and (b) equivalent circuit of the double-loop.

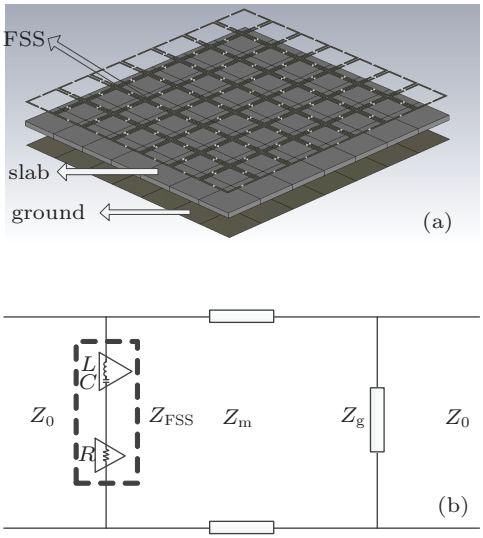


Fig. 3. (a) A three-dimensional (3D) view of the absorber, and (b) equivalent circuit of the absorbers' configuration.

The array of thin and conducting narrow strips has either capacitive or inductive impedance. If the tangential component of the incident electric field is parallel to the conductors, the reactance is inductive as depicted in Fig. 1(a) and *vice versa* as depicted in Fig. 1(b). The immittance expressions of the strip grating were given for both TE incidence and TM incidence[23]

$$\frac{X_{\rm TE}}{Z_0} = F(p,w,\lambda) = \frac{p\cos(\theta)}{\lambda}\left[\ln\csc\left(\frac{\pi w}{2p}\right)+G(p,w,\lambda,\theta)\right], \quad (1)$$

$$\frac{X_{\rm TM}}{Z_0} = F(p,w,\lambda) = \frac{p\sec(\phi)}{\lambda}\left[\ln\csc\left(\frac{\pi w}{2p}\right)+G(p,w,\lambda,\phi)\right], \quad (2)$$

where θ/ϕ is the angle of incidence, λ is the wavelength in the air and

$$G(p,w,\lambda,\theta) = \frac{1}{2}\times\frac{(1-\beta^2)^2\{(1-\beta^4/4)(A_+ + A_-)+4\beta^4 A_+ A_-\}}{(1-\beta^4/4)+\beta^2(1+\beta^2/2-\beta^4/8)(A_+ + A_-)+2\beta^6 A_+ A_-}. \quad (3)$$

In the above expression,

$$A_\pm = \frac{1}{\sqrt{(1\pm\frac{2p\sin(\theta)}{\lambda}-\frac{p\cos(\theta)}{\lambda})^2-1}} \quad (4)$$

and $\beta = \sin(\pi w/2p)$. The susceptance can be obtained as follows:

$$\frac{B_{\rm TE}}{Y_0} = 4F(p,d,\lambda) = \frac{p\sec(\theta)}{\lambda}\left[\ln\csc\left(\frac{\pi w}{2p}\right)+G(p,d,\lambda,\theta)\right], \quad (5)$$

$$\frac{B_{\rm TM}}{Y_0} = 4F(p,d,\lambda) = \frac{p\cos(\phi)}{\lambda}\left[\ln\csc\left(\frac{\pi w}{2p}\right)+G(p,d,\lambda,\phi)\right]. \quad (6)$$

According to the expressions presented above, the admittances of the single-square loops (SSL) and double-square loops (DSL) are given respectively as follows:

$$Y_{\rm SSL} = \frac{1}{R_1+{\rm j}wL_1+\frac{1}{{\rm j}wC_1}}$$

$$= \frac{1}{R_1 + \mathrm{j}X_1 + \dfrac{1}{\mathrm{j}B_1}}, \tag{7}$$

where $B_1 = wC_1 = 4F(p,g,\lambda)\cdot(d/p)$ and $X_1 = wL_1 = F(p,2w,\lambda)\cdot(d/p)$. The value of R_1 is half of the inserted resistors.

$$Y_{\mathrm{DSL}} = \frac{1}{R_1 + \mathrm{j}wL_1 + \dfrac{1}{\mathrm{j}wC_1}} + \frac{1}{R_2 + \mathrm{j}wL_2 + \dfrac{1}{\mathrm{j}wC_2}} = \frac{1}{R_1 + \mathrm{j}X_1 + \dfrac{1}{\mathrm{j}B_1}} + \frac{1}{R_2 + \mathrm{j}X_2 + \dfrac{1}{\mathrm{j}B_2}}, \tag{8}$$

where

$$B_1 = wC_1 = 0.75B_{1p}\cdot\frac{d_1}{p}, \quad B_2 = wC_1 = \frac{B_{1p}B_{2p}}{B_{1p}+B_{2p}}\cdot\frac{d_2}{p},$$

$$X_1 = wL_1 = \frac{X_{1p}X_{2p}}{X_{1p}+X_{2p}}\cdot\frac{d_1}{p}, \quad X_2 = wL_2 = F(p,2w_2,\lambda)\cdot\frac{d_2}{p},$$

$B_{1p} = 4F(p,g_1,\lambda)$, and $B_{2p} = 4F(p,g_2,\lambda)$. The values of R_1 and R_2 are, respectively, the half of the outer inserted resistors and inner inserted resistors.

In the following discussion, results brought into comparison will be given for the validations. In Table 1, resonant frequencies predicted by EC-FDTD[24,25] codes and by our EC method are compared for the single-square loops with zero resistance.

Table 1. The simulated results for single-square loops by EC-FDTD and by the EC methods.

Dimensions/mm				Results/GHz	
p	w	d	g	EC-FDTD	EC
5.25	0.47	5.0	0.25	16.05	15.8
4.35	0.3	4.07	0.28	19.5	18.9
5.0	0.28	4.6	0.4	17.5	16.5

In Table 2, resonant frequencies predicted in Ref. [21] and by the EC method are compared for the double-square loops with zero resistance. In the table, f_1 and f_2 are reflection frequencies, while f_{T} represents transmission frequency. These two results are slightly different because of the presence of 0.027-mm polyester substrate in the calculation of Ref. [21].

Table 2. The results of Ref. [21] and the EC-based calculations for double-square loops.

Dimensions/mm							Results/GHz					
p	w_1	d_1	g_1	w_2	d_2	g_2	$f_1(20)$	f_1(EC)	$f_{\mathrm{T}}(20)$	f_{T}(EC)	$f_2(20)$	f_2(EC)
5.0	0.17	4.83	0.17	0.17	3.50	0.50	11.5	12.1	17.5	18.1	24.5	24.7
5.0	0.17	4.83	0.17	0.17	3.00	0.75	11.5	12.1	20.0	20.5	29.8	29.4
5.0	0.17	4.83	0.17	0.17	2.50	1.00	11.5	12.1	24.0	23.6	35.7	28.9
5.0	0.17	4.57	0.43	0.17	3.35	0.44	14.6	15.2	20.2	20.7	26.8	15.8
5.5	0.20	5.00	0.40	0.34	2.63	1.04	13.4	14.0	25.0	24.8	38.5	35.4

2.2. Calculation and comparison

Figure 3 reports the configuration of the absorbers. Once the impedances of the FSS loaded with the resistors are derived, the reflection coefficients Γ and the transmission coefficients τ can be calculated according to the classical transmission line approach[26,27]

$$\Gamma = \frac{AZ_0 + B - CZ_0{}^2 - DZ_0}{AZ_0 + B + CZ_0{}^2 + DZ_0},$$

$$\tau = \frac{2Z_0}{AZ_0 + B + CZ_0{}^2 + DZ_0},$$

where A, B, C, D represent the terms of the $ABCD$ matrix of the absorbers:

$$\begin{pmatrix} A & B \\ C & D \end{pmatrix} = \begin{pmatrix} 1 & 0 \\ Y_{\mathrm{fss}} & 1 \end{pmatrix} \begin{pmatrix} \cos(\beta_m d) & \mathrm{j}Z_m \sin(\beta_m d) \\ \dfrac{\mathrm{j}\sin(\beta_m d)}{Z_m} & \cos(\beta_m d) \end{pmatrix} \begin{pmatrix} 1 & 0 \\ Y_{\mathrm{g}} & 1 \end{pmatrix}.$$

In the above equations, $Y_{\mathrm{fss/g}}$ is the admittance. Other parameters can be obtained as follows: $Z_m^{\mathrm{TE}} = w\mu/\beta_m$, $Z_m^{\mathrm{TM}} = \beta_m/w\varepsilon$, $\beta_m = \sqrt{k_m^2 - k_t^2}$, $k_t = k_0\sin(\theta)$, and $k_m = k_0\sqrt{\varepsilon_r\mu_r}$.

The present approach can be employed to predict the performance of the absorbers. Three different FSSs are printed on a grounded slab with the same thickness (5.3 mm) and permittivity (2.25). In Fig. 4, the reflection coefficients computed by our EC method, by EC-FDTD, and by the commercial software HFSS are compared. In this example, the HFSS takes 104 s to finish the simulation while our EC method only takes 2 s. This structure can absorb 5-dB electromagnetic energy in the band from 5 GHz to 15 GHz. The three simulated results agree well. The same kind of structure depicted in Fig. 5 with different dimensions from the previous ones in Fig. 4 is simulated by the same methods. In this verification, 123 s and 2 s are respectively cost by HFSS and our EC method. From the comparison shown in Fig. 5, the EC method can approximately predict the performance of the absorbers with the absorbing band from 5 GHz to 14 GHz. In Fig. 6, we show the reflection coefficients for double-square loops. The absorbers obtain a good performance (-10 dB in the frequency range 5 GHz–12.5 GHz) from the EC method, which is much faster than the HFSS method (more than 20 times faster). The results based on the EC method are approximately consistent with those by EC-FDTD codes and by HFSS. We present the results here in order to verify the performance of the EC method, which are not the optimal ones to absorb the incoming power. From these

three examples, the three simulated results have discrepancy at higher frequency in the band. One reason is that the equivalent circuit model is valid for wavelengths and angles of incidence θ in the range $p(1+\sin(\theta))/\lambda < 1$. In this condition, the incoming power cannot be redirected in other directions, but dissipated by the lumped resistors. The frequency range for utilizing the EC method is limited by this condition for a fixed unit cell. Other reasons will be discussed in the next section.

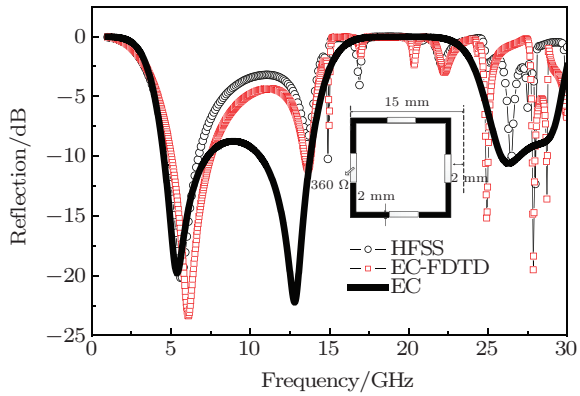


Fig. 4. (color online) The simulated reflection coefficients for SSL by three different methods.

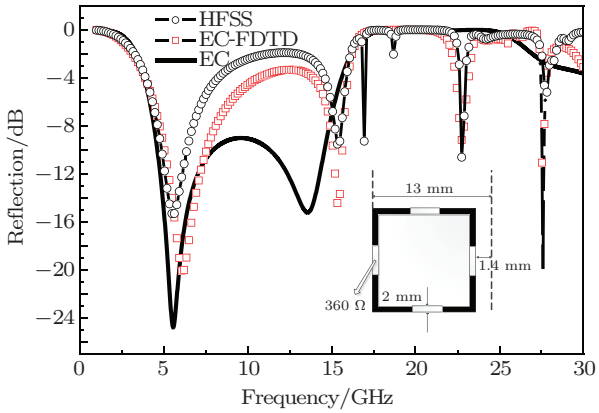


Fig. 5. (color online) The simulated reflection coefficients for SSL by the equivalent circuit model, HFSS, and EC-FDTD codes.

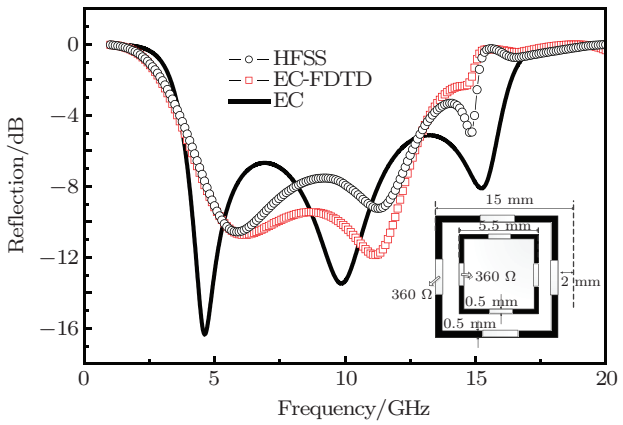


Fig. 6. (color online) The simulated reflection coefficients for DSL by three different methods.

3. Designs and measurements

In order to verify the proposed equivalent circuit method, two experimental prototypes are designed by the EC method combined with the genetic algorithm in this paper. Furthermore, these two designs are manufactured and measured. We tested these two absorbers' performance in a microwave anechoic chamber as shown in Fig. 7. An agilent vector analyzer E8363A with the frequency band between 45 MHz and 40 GHz is adopted. Two broadband horn antennas (ETS·LINDGREN) with the band from 1 GHz to 18 GHz are utilized. Due to the grounded plane, the reflection coefficients of the absorbers represent the absorbtion and are normalized with respect to the grounded plane without lumped elements and substrate. Each design was fabricated on an F_4B substrate, and FSSs were fabricated using standard optical lithography.

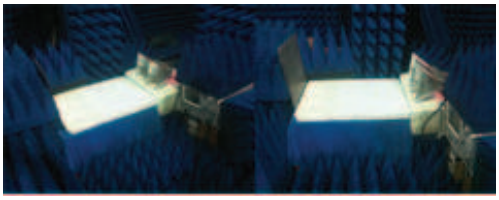


Fig. 7. (color online) Schematic plot of reflection measurement.

3.1. Single-square loop

A part of the first sample with 24 by 35 single-squares loops printed on an F_4B substrate ($\varepsilon_r = 2.25$, $\delta = 0.001$, and $h = 5.3$ mm) is shown in Fig. 8. The parameters are $p = 10$ mm, $d = 9.6$ mm, $w = 0.5$ mm as defined in the paper.[19] The inserted resistors have the value of 390 Ω. Three results including simulated ones by EC-FDTD codes, computed ones by EC method, and the experimental ones are depicted in Fig. 8. It can be seen that the experimental results (dashed line with green circle) match well with simulated ones by both EC-FDTD codes (dashed line with red rectangle) and the EC method (dashed line), and we can conclude that this configuration has an absorbing band from 6 GHz to 14 GHz. The effective absorbing range exists in a wide frequency range.

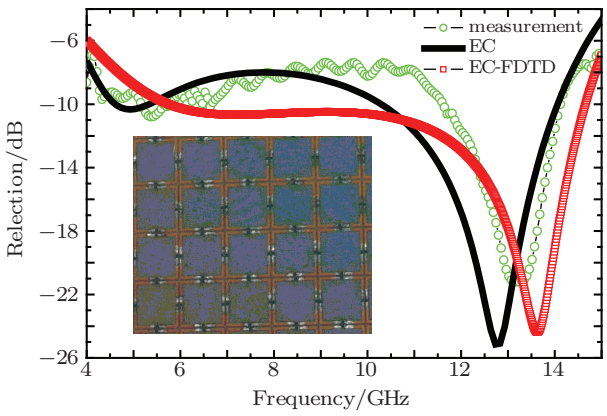


Fig. 8. (color online) The reflection coefficients for SSL.

The slight discrepancy of the results can be ascribed to the fabrication error, such as fake soldering between metal FSS and the lumped resistors. The results indicate that inserted resistors lead to the enhancement of the bandwidth of the absorbers.

3.2. Double-square loop

The second sample is 24 by 35 double-squares loops printed on an F_4B substrate ($\varepsilon_r = 2.25$, $\delta = 0.001$, and $h = 5.3$ mm). The parameters are $p = 10$ mm, $d_1 = 9.6$ mm, $d_2 = 5.5$ mm, $w_1 = 0.5$ mm, and $w_2 = 0.5$ mm. The inserted resistors have the value of 390 Ω for both outer and inner loops. The three results defined in Subsection 3.1 are depicted in Fig. 9. From 4.5 GHz to 14 GHz, the simulated absorption by EC-FDTD is more than 10 dB, and the simulated one by the EC method and the measured one are around 8 dB. Apparent discrepancy can be seen from these results in high frequencies. One reason except for fabrication error, another reason might be the mutual coupling between cells of the absorbers, which is ignored in the simulated analysis. In addition, in both full-wave analysis and EC calculations, we only set resistance, while a parallel RLC circuit should be taken into account for a lumped resistor especially in higher frequency ranges. As highlighted in the previous subsection, the results indicate that lumped resistors have a great influence on the absorbing properties. Compared with single-square loops, adding inner loops can broaden the absorbing frequencies range in lower frequency. However, the outer loop of each cell makes the main contribution.

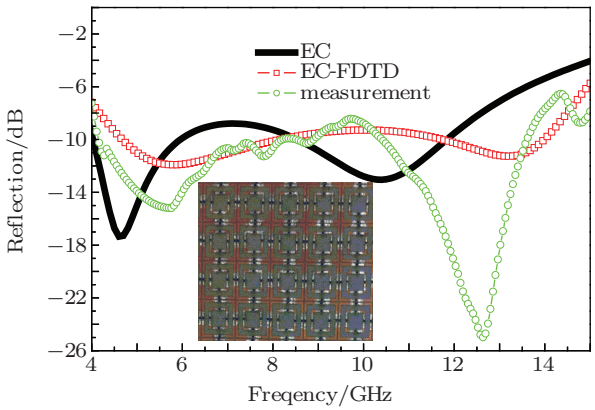


Fig. 9. (color online) The reflection coefficients for DSL.

4. Conclusion and expectation

A novel design named equivalent circuit method (EC) for absorbers has been presented in this paper. It can give a fast and accurate prediction for the configuration. By using the method, two different structures are designed. One has the absorbing frequency band from 6 GHz to 14 GHz and the other one has the band from 4.5 GHz to 14 GHz. The feasibility of the EC method for the absorbers is demonstrated by these experimental prototypes. As highlighted in Subsection 2.2, choosing a suitable FSS unit cell, which resonates well before the grating lobes when FSS period is larger than one wavelength, is important in order to apply the EC method.

A frequency selective radome with the absorbers attracts us, which acts like a passband filter to improve the appearance of the antenna in the operating frequency range, while behaving as absorbers to reduce the radar cross section at other bands. Its design is of importance in both reducing the radar cross section for antennas and improving the appearance of antenna. The equivalent circuit method can give a great and fast help to design this radome. This work will be reported later.

Acknowledgements

The authors acknowledge Filippo Costa in University of Pisa for valuable help and professor T. Liebig in Duisburg–Essen University for giving advice on EC-FDTD codes. We also acknowledge Prof. Cui Tie-Jun and Dr. Shen Xiao-Peng for their help on understanding metamaterial absorbers.

References

[1] Agrawal V and Imbriale W 1979 *IEEE Trans. Antennas Propag.* **27** 466
[2] Wu T K 1994 *IEEE Trans. Antennas Propag.* **42** 2369
[3] Munk B A 2000 *Frequency Slective Surfaces — Theory and Design* (New York: John Wiley & Sons)
[4] Gustafsson M and Karlsson A 2006 *IEEE Trans. Antennas Propag.* **54** 1897
[5] Saleh A A M and Semplak R A 1976 *IEEE Trans. Antennas Propag.* **24** 780
[6] Pelton E L and Munk B A 1974 *IEEE Trans. Antennas Propag.* **22** 799
[7] Sievenpiper D, Zhang L, Broas R F J, Alexopolous N G and Yablonovitch E 1999 *IEEE Trans. Microwave Theory Techniques* **47** 2059
[8] Costa F, Gempvesi S and Monorchio A 2009 *IEEE Antennas Wireless & Propagation Lett.* **8** 1341
[9] Landy N I, Sajuyigbe S, Mock J J, Smith D R and Padilla W J 2008 *Phys. Rev. Lett.* **100** 207402
[10] Wang X D, Ye Y H, Ma J and Jiang M P 2010 *Chin. Phys. Lett.* **27** 94101
[11] Yang Y J, Huang Y J, Wen G J, Zhong J P, Sun H B and Oghenemuero G 2012 *Chin. Phys. B* **21** 038501
[12] Gu C, Qu S B, Pei Z B, Xu Z, Liu J and Gu W 2011 *Chin. Phys. B* **20** 017801
[13] Yuan J and Shen Z X 2007 *IEEE Antennas Wireless & Propagation Lett.* **6** 1536
[14] Costa F, Monorchio A and Manara G 2012 *IEEE Trans. Antennas Propag.* **54** 35
[15] Costa F and Monorchio A 2012 *IEEE Trans. Antennas Propag.* **60** 2740
[16] Shen X P, Cui T J, Zhao J M, Ma H F, Jiang W X and Li H 2011 *Opt. Express* **19** 9401
[17] Marcuvitz N 1951 *Waveguide Handbook* (New York: McGraw-Hill)
[18] Anderson I 1975 *Bell System Technical Journal* **54** 1725
[19] Langley R J and Drinkwater A J 1982 *IEE Proceedings H — Microwaves Optics and Antennas* **129** 1
[20] Langley R J and Parker E A 1982 *Electron. Lett.* **18** 294
[21] Langley R J and Parker E A 1983 *Electron. Lett.* **19** 675
[22] Lee C K and Langley R J 1985 *IEE Proceedings H — Microwaves Optics and Antennas* **132** 395
[23] Yilmaz A E and Kuzuoglu M 2009 *Radio Engineering* **18** 95
[24] Renings A, Otto S, Caloz C, Lauer A, Bilgic W and Waldow P 2006 *Int. J. Numer. Model.* **19** 141
[25] Rennings A, Otto S, Lauer A, Caloz C and Waldow P 2006 *Proc. European Microwave Association* **2** 71
[26] Wu X H, Kishk A A and Glisson A W 2006 *IEEE Trans. Antennas Propag.* **54** 2731
[27] Costa F and Monorchio A 2011 *PIER* **111** 467